Building and Environment 243 (2023) 110694

Contents lists available at ScienceDirect

Building and Environment

journal homepage: www.elsevier.com/locate/buildenv

Worldwide potential of emissive materials based radiative cooling technologies to mitigate urban overheating

Laura Carlosena [a,*], Álvaro Ruiz-Pardo [b], Enrique Ángel Rodríguez-Jara [b], Mattheos Santamouris [c]

[a] Engineering Department, Public University of Navarre (UPNA), Campus de Arrosadía, 31006, Pamplona, Spain
[b] Departamento de Máquinas y Motores Térmicos, University of Cadiz, Av. University of Cadiz 10, 11519, Cádiz, Spain
[c] High Performance Architecture, School of Built Environment, University of New South Wales, Sydney, NSW, 2052, Australia

ARTICLE INFO

Keywords:
Radiative cooling
Urban heat island
Radiant heat transfer
Worldwide
Cooling potential

ABSTRACT

Radiative cooling has gained significant attention in recent years for its passive heat evacuation capabilities. Numerous materials have been developed, but comparing their cooling effectiveness has proven challenging due to inconsistent experimental conditions. This study aims to bridge this gap by evaluating the heat evacuation potential of various radiative cooling materials under consistent climatic conditions.

Using a validated heat transfer model, the performance of eleven materials was simulated in twenty-two Urban Overheating-affected cities. The assessment considered factors such as radiated heat losses, solar heat gains, and convective heat losses to gauge the cooling power of each material. The simulation assumed an active system where the materials were placed on a highly conductive, uninsulated surface, akin to having a fluid at a constant temperature beneath.

The ability of materials to radiate heat and cool down depends on their optical properties. The findings suggest limited benefits in equatorial climates, with an average monthly total heat exchanged (MATHE) of −19.73 $kWhm^{-2}$. Materials displayed consistent behavior throughout the year in climates with high relative humidity levels. Climates with elevated ambient temperatures derived the greatest advantages from strictly selective and highly reflective materials that emitted within the atmospheric window. Arid climates showed potential during transition times (MATHE -74.5 $kWhm^{-2}$), while warm temperate climes benefited during summer months (MATHE -112.1 $kWhm^{-2}$). In snow zone climates, the system could be utilized year-round for cooling-intensive scenarios, with a MATHE of −203.8 $kWhm^{-2}$. This study evaluates radiative cooling materials' effectiveness in different climates, informing energy-efficient cooling applications.

1. Introduction

The emissions of CO_2 due to the burning of coal, oil, and gas have continuously increased and are believed to lead to global warming and rising sea levels [1]. According to the International Energy Agency (IEA), cooling accounts nowadays for 20% of the total electricity used in buildings around the world, and this tendency is predicted to increase in the hottest areas of the world with the demand for greater thermal control, population growth, and climate change [2]. The most widespread system of air conditioning (AC) is based on vapor compression. This kind of air conditioning discharges latent waste heat to the ambient air. It has shown an increase in the street air temperature in central Paris's urbanized areas, ranging from 0.5 °C to 2 °C depending on the AC equipment employed [3]. The cooling demand increases notably with heatwaves, where the situation worsens by the use of air conditioning equipment, leading to large energy consumption and augmenting outdoor heat stress [4]. AC systems release heat into the street, warming the outside air and increasing the heatwave [3,5]. During the hot spell of 2018 in Beijing, 50% of the power capacity went to air conditioning [6].

Extensive urban expansion and population growth have aggravated environmental problems such as local climate, resource depletion, and air pollution change [7]. Envelope materials of buildings and urban structures significantly influence the urban thermal balance; they absorb solar and infrared radiation and evacuate part of the accumulated heat to the ambient air and atmosphere increasing ambient temperature [8]. The effects of higher temperature on energy, health, pollution, and

* Corresponding author.
E-mail address: laura.carlosena@unavarra.es (L. Carlosena).

https://doi.org/10.1016/j.buildenv.2023.110694
Received 20 June 2023; Received in revised form 1 August 2023; Accepted 1 August 2023
Available online 5 August 2023

vulnerability could be aggravated depending on the emissions' path model and the technological, socioeconomic, and demographic developments [9]. The climate conditions of a specific location will significantly impact the cooling demands and the cooling potential.

Urban heat island (UHI) is a phenomenon that occurs in cities and refers to the increase in temperature in urban areas compared to nearby rural areas. UHI is highly interlinked to amplified cooling loads during the summer period [10]. The average UHI varies between 0.5 °C and 7 °C, where 90% of the data is below 4.5 °C [9]. The magnitude of UHI varies in Asian and Australian cities from 0.5 °C to 11 °C [11] and between 1 °C and 10 °C in Europe [12]. On the other hand, the UHI and heatwaves have a relevant environmental and financial impact, especially on vulnerable and low-income populations [13].

Moreover, exposures to high ambient temperature represent a severe health danger [14]. An augment of the mean surface temperature by 1 °C caused a 32% increase in the odds of death from heat exposure in Phoenix, Arizona [15]. The effect on health has a greater toll on the elderly, a recent study on heat-specific deaths in Spain showed that up to 62% of the deceased were over 65 years old [16].

To lower urban temperatures by avoiding traditional heat-absorbing materials, solutions with high albedo have been proposed, such as cool materials [17], greenery [18,19], and phosphorescent materials [20,21]. More recently, daytime radiative cooling materials have been proposed as a mitigation strategy for the Urban Heat Island as a passive technique. There are some precedents of savings simulations using new materials for radiative cooling [22–25]. Nevertheless, when used as building coatings (passive approach), daytime radiative cooling materials might lead to heat penalties during the winter [26]. A recent paper already calculated the overcooling penalty, the decrease in net inflow radiation was 354.9 Wm^{-2} in Kolkata [27]. On the other hand, a numerical study showed that using materials that could modulate their reflectivity and emissivity increased the maximum net radiation inflow by 51.5 Wm^{-2}, leading to heating the cities during the winter [28].

This research pretends to establish the first approach in calculating the radiative cooling power of existing developed materials and theoretical materials. The first kind were produced and tested in the literature, whereas the theoretical materials are ideal materials that do not currently exist. They have assigned emissivity values of zero or non-zero to different wavelengths. In our case, they have zero emissivity values in the solar wavelengths and the non-zero emissivity values centered in the transparency window of the atmosphere. This assumption allows to calculate an optimal case, as the materials emit highly around the atmospheric window without absorbing solar radiation in the solar range. Moreover, the following aspects are considered:

a) Realistic weather conditions across the globe throughout the year. One common drawback detected among the literature [29–32] is that to evaluate the daytime radiative cooling potential, authors assume clear sky conditions. Clouds can act as an insulation barrier preventing a surface from losing its heat since the atmosphere re-radiates the emitted energy back towards the source. The increase of atmospheric emissive spectral irradiance in the sky window leads the radiative cooler to absorb more atmospheric radiation and restrains its cooling performance [33].
b) Spectral selectivity of the materials in 39 bands. The energy model [34] considers the material's spectral selectivity, the incoming spectral solar, and atmospheric radiation.
c) The application of radiative cooling materials as building coatings may lead to excessive cooling penalties in buildings during winter. The purpose of these simulations was to determine the maximum amount of heat that could be effectively removed by the system. Integrating these materials into an air conditioning system could enhance efficiency, reduce energy consumption, and minimize heat dissipation into the surrounding environment. However, it should be noted that the system has not been implemented in a specific building, as doing so would require more intricate thermal considerations. The configuration of the simulated system is as follows: the materials under study are fixed on the upper face of a highly conductive surface in direct contact with a fluid at 25 °C. The upper face is free to the atmosphere to dissipate the heat. This configuration is assimilated to an active air conditioning solution. Some research has already integrated these materials on active systems [22,23,29,35]; however, before doing so, the materials' potential as active systems should be studied independently of the application system.
d) Different climates of applications. Radiative cooling heat exchange is a renewable energy and a free cooling source, as such, the location is crucial to determine the potential. To determine the influence of climate in the ability to evacuate heat, we study the materials' response in twenty-two cities with urban overheating distributed in fourteen different climates.

As a result of the research, considerations for choosing the appropriate material are given for each city and climate. This study's main novelty is the potential cooling comparison of different daytime radiative cooling materials across the most critical world climates and specifies the contribution of each heat transfer.

2. Methodology

The research followed the next steps to obtain the monthly accumulated heat of several daytime radiative cooling materials under different climates. First, the Köppen-Geiger climate classification's central global climates were selected according to their prevalence that was determined by the number of settlements located in that climate. For each climate, at least one representative city that suffers from urban overheating was chosen. Secondly, ten radiative cooling materials were selected, two from the literature (RC1 and RC2), four theoretical materials (M5 to M8), recently developed low-cost radiative materials (AS_2.2, AS_2.3, V_1.1, and V1.2) [36], and a bare aluminum substrate (A) for comparison purposes. We selected a non-emissive aluminum as it was tested alongside the low-cost developed materials. The simulations considered the entire year as some locations might need cooling outside the summer solstice. The monthly accumulated heat by each heat transfer mechanism was calculated for every material in every city, using the previously developed and validated heat transfer model [34] that considered cloud coverage through the cloudiness factor (0–1). Finally, the results were compared according to their radiated heat. Moreover, the conclusions, suitability, and limitations for each material and climate are drawn.

2.1. Model setup

As previously mentioned, an active application (Fig. 1) was simulated. The radiative cooling materials were placed on top of a very conductive surface with a heat source at a constant temperature, the system considered no insulation. Below the material, the temperature is 25 °C, the exterior heat transfer coefficient is based on a linear expression from ESP-r [37] that considers the surface's temperature, the ambient air temperature, the wind speed, and the interior heat transfer coefficient is (1000 $W\ m^{-2}\ K^{-1}$). The set temperature and heat transfer coefficient were chosen as follows. On the one hand, comfort temperatures inside buildings during the cooling period are around 25 °C. Therefore, it is the selected temperature for the liquid that flows below the radiative surface. On the other hand, the selected heat transfer coefficient is a typical value for a liquid (water) flowing through a pipe in forced convection [38].

The results show the monthly energy exchanged ($kWh{\cdot}m^{-2}$), by the surface with its surroundings and discriminated in the following terms: 1) Heat evacuated by radiation, 2) Heat absorbed due to the incidence of solar radiation and longwave radiation, 3) heat exchanged by convection with the air and 4) Total heat exchanged between the surface and

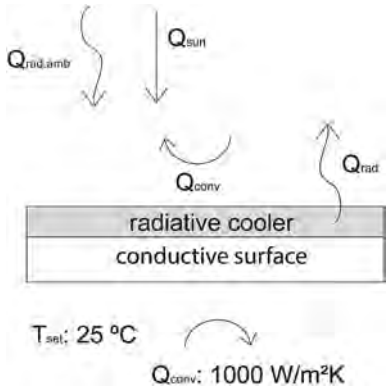

Fig. 1. Active system assimilation.

the environment, i.e. the sum of the first three terms and which coincides, by conservation of energy, with the heat exchanged by convection between the plate and the water flowing underneath it. As a result, the general balance on the surface:

$$q_{cd} = q_{rad} + q_{sun} + q_{conv} \tag{1}$$

Where: q_{cd} is the conduction heat, q_{rad} the heat exchanged by radiation with the exception of that absorbed by solar radiation, q_{sun} heat generated by absorbed solar energy, q_{conv} the heat exchanged by convection, and the term q_{rad} includes the radiant exchange in the 39 bands indicated above. It is calculated as the sum of the exchange in each of the bands:

$$q_{rad} = \sum_{\Delta v_i} q_{r,s,\Delta v_i} \tag{2}$$

Where the heat exchanged in each band is:

$$q_{r,s,\Delta v_i} = -\int_{v_i}^{v_j} \varepsilon_s(v)\left(E_b(v,T_s) - \varepsilon_{sky}(v)E_b(v,T_{air})\right)dv \tag{3}$$

And where each of the terms in the above equation are, $q_{r,s,\Delta v_i}$ heat exchanged by radiation in band "i", v_i initial wavenumber of the "i" band, v_j end wavenumber of the "i" band, $\varepsilon_s(v)$ surface emissivity for wavenumber "v", $\varepsilon_{sky}(v)$ sky emissivity at wavenumber "v", $E_b(v,T_s)$ emissivity of a black body at surface temperature for wavenumber "v", and $E_b(v,T_{air})$ emissivity of a black body at air temperature for wave number "v".

2.2. City selection criteria

To determine the worldwide potential application of radiative cooling, the climates of application were studied. The climates that encompass the highest number of settlements around the world were analyzed. Oke [39] demonstrated the existing relationship between an urban settlement's size and the magnitude of its heat island. Radiative cooling is of particular interest in cities suffering from urban overheating, as it could alleviate part of the excess heat. Radiative cooling materials reject heat through the atmospheric window, and as a result, do not contribute to increasing the temperatures in the surroundings.

The climate selection and representative cities resulted from combining the information from the Global Urban Heat Island Dataset [40] and the Köppen-Geiger classification by coordinates [41]. The Köppen-Geiger climate classification was selected as it considers humidity, which is a determinant factor for radiative cooling rates and potential; moreover, it is widely used in research. As a result, the relationship between the number of settlements, population, and climates was established. Fig. 2 shows the complete dataset distribution with a total of 31,500 locations. Cities that showed higher temperatures than rural areas during the day (positive daytime temperature difference) and during the night (positive nighttime temperature difference) were prioritized. As a result, Fig. S2 shows the number of settlement distribution for all the cities in the data set, cities with more than 5000 inhabitants and positive daytime and nighttime temperature, and cities with more than 3 million inhabitants and positive daytime and nighttime temperature (90 locations that represent 0.003% of the initial data). Secondly, considering the unfiltered data, with 31,500 locations, climates that grouped less than 2% of the total settlements such as Bwk and Csb were not considered. This resulted in a total of 86 locations that complied with the criteria.

The only exception was BSk, whose representativity was not consistent with population increase of up to 3 million inhabitants; nevertheless, 2.4% of cities with 1,000,000 population and positive thermal daytime and nighttime temperature difference were under this climate. Moreover, to select one representative city for each climate, locations with higher daytime and nighttime temperature differences were favored (Fig. S1). The final city selection was done prioritizing cities with reported urban overheating. For climates that grouped a high number of settlements, two cities were selected. The resulting city selection is presented in Table S1 and shown in Fig. 3.

Beside results on the heat transfer, information regarding the climate was calculated, such as the monthly mean of the daily maximum air temperature (°C), the monthly mean of the air temperature (°C), the monthly mean of the daily minimum air temperature (°C), monthly mean incident radiation ($W{\cdot}m^{-2}$) and monthly mean relative humidity (%). The climate data of the cities were obtained from Meteonorm [42] using the standard irradiation model, the standard temperature model, and the included radiation model [43]. The typical meteorological year type of file was used (.tm2) with hourly data and solar time. The ambient temperature, solar radiation, sky cover, relative humidity, and wind speed were used to calculate the materials' cooling potential.

2.3. Optical properties of the materials

Different radiative cooling materials were selected to determine the radiative cooling potential and compared to a common construction material such as aluminum (A). Fig. 4 shows the materials' spectra discretized per wavelength band and grouped by type of material. Ideal theoretical materials are very reflective in the solar wavelengths and very emissive in the atmospheric window (8–13 μm), marked as vertical point lines in the graphs. The difference among the different theoretical materials is the amplitude of the emissivity band along the atmospheric window (Fig. 4a, b, c, and d). Besides, several materials tested in the literature were selected, a photonic radiative cooler that emits highly in the atmospheric window and a randomized glass polymer metamaterial, which is a broadband emitter (Fig. 4e and f, respectively). Finally, several low-cost radiative coolers based on aluminum with an emissive (Fig. 4j and k) and others based on an enhanced solar reflector (Fig. 4h and i) were simulated as well.

3. Results

In this section the different results of the simulations are presented. To summarize the main findings, maps and boxplots were presented. To present this information, among the different types of radiative cooling material we selected one representative material: aluminum with an emissive layer with peaks of emissivity in the atmospheric window (AS_2.3), a low-cost broadband emitter (VS_1.1), a strictly selective theoretical material (M8), and a broadband emitter (RC2). First, the map shows the total heat (Fig. 5) for the months of June and December. Secondly, Figs. 6–8 show the simulation boxplots results for those same materials. Boxplots were selected as they provide a visual summary of a dataset by displaying the distribution, median (horizontal bar dividing the box), the box goes from the 25th to the 75th percentile, and the

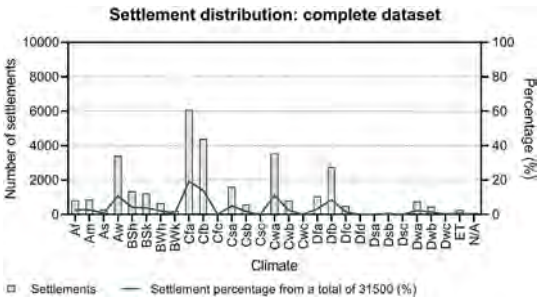

Fig. 2. Prevalence per climate, includes all the information in the dataset.

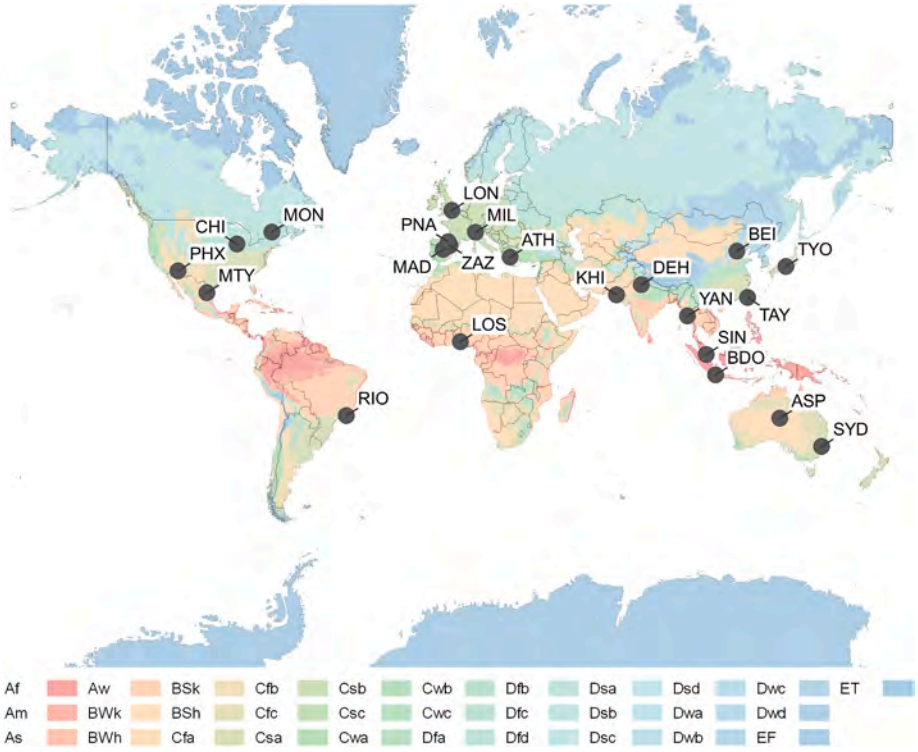

Fig. 3. Map of the city selection above the Köppen-Geiger classification.

whiskers, go down to the smallest value and up to the largest, making it easier to understand the overall spread and central tendency of the data. The shorter the boxplot is the more uniform the behavior is throughout the year; on the other hand, the taller it is the more it changes throughout the year. In each figure, the monthly accumulated heat variation for every city arranged by climate (Figs. 6–9) is shown; graphs show the radiated heat losses, the solar heat gains, the convective heat gains or losses, and the total accumulated heat variation.

The detailed results are given in different subsections grouped by climate zone: equatorial (A), arid (B), warm temperate (C) and snow (D). The monthly accumulated radiated heat and the monthly accumulated total heat for each material and location are shown. The sign criterion considers positive values for heat gains and negative values for heat losses, so the lower the number is, the higher the effective cooling is. The monthly climate data are presented in the Supplementary Material Fig. S3 to Fig. S7.

3.1. Equatorial zone climates (A)

The equatorial rainforest's fully humid climate (Af) is characterized by minimum precipitation above 60 mm on the driest month; Bandung and Singapore were the representative cities. When considering all materials, the monthly accumulated energy exhibits minimal variation across the months, reflecting the consistent climate patterns throughout the year (Fig. 10a and b). The system demonstrated effective heat dissipation capabilities in Bandung but not in Singapore (Fig. 10g). This disparity can be attributed to Singapore's higher average ambient temperatures, higher solar radiation levels throughout the entire year as well as increased cloud cover. The ability to evacuate heat is greatly influenced by the capacity to radiate heat. In this case, all the materials radiated more energy in Bandung (Fig. 10f). Notably, materials RC2, M8, V_1.1, V_1.2 (broadband emitters) exhibited significant heat radiation in Bandung while A, AS_2.2 and 2.3 demonstrated nearly identical performance. In Bandung monthly mean of the total heat for VS_1.1, RC2, and M8 was −33.73, −52.9, and −62.1 $kWhm^{-2}$, respectively (Fig. 10a). However, in Singapore, the heat gains surpassed the heat

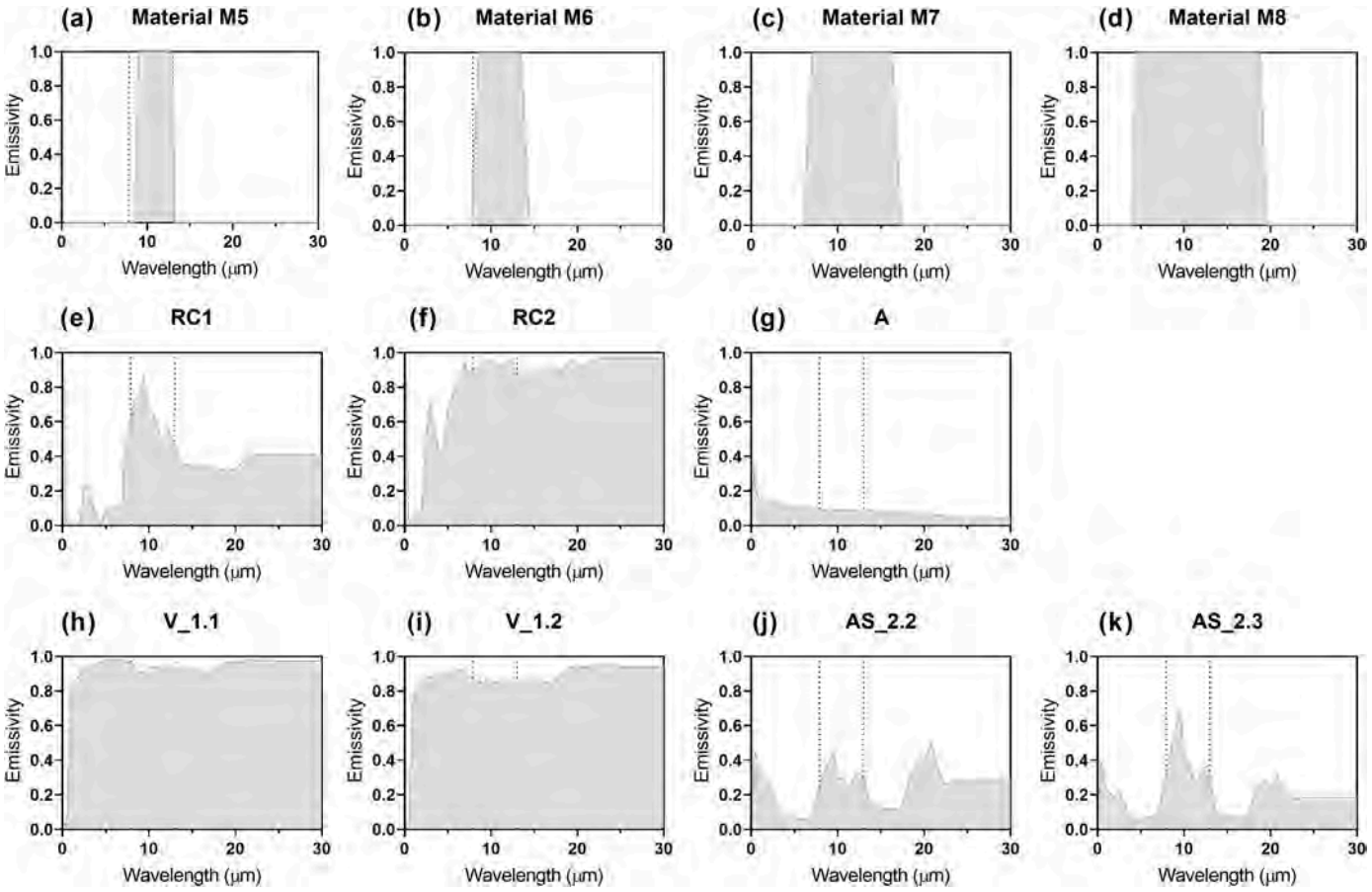

Fig. 4. Emissivity spectra of theoretical materials: (a) M5, (b) M6, (c) M7, and (d) M8; emissivity spectra of radiative cooling materials from the literature (e) RC1 [30] and (f) RC2 [32]; emissivity spectra of (g) A (aluminum), emissivity spectra of samples with Vikuiti and an emissive coating (h) V_1.1 and (i) V_1.2); and of aluminum with an emissive coating (j) AS_2.2 and (k) AS_2.3.

losses being the most notable in May, where the heat gains reached up to 43 $kWhm^{-2}$ for V_1.1, 19.3 $kWhm^{-2}$ for RC2, 8.1 $kWhm^{-2}$ for M8 (Fig. 10b). This result can be explained because during May, the ambient temperature in Singapore was 28 °C, which was 3 °C above the system's operational temperature of 25 °C.

The equatorial rainforest climate (Am) selected representative city is Yangon. The system was unable to evacuate heat except when the system used the theoretical material M8, which showed low potential for heat evacuation during January (-20.8 $kWhm^{-2}$), June (-8 $kWhm^{-2}$), and December (-13 $kWhm^{-2}$) (Fig. 10c). The materials' ability to radiate heat demonstrated substantial variations throughout the year, particularly for broadband materials with high solar reflectance (Fig. 10f). Conversely, materials AS_2.2 (-7.9 $kWhm^{-2}$), AS_2.3 (-10 $kWhm^{-2}$), and A (mean −2.1 $kWhm^{-2}$), which were characterized by moderate reflectivity and emissivity, exhibited consistent heat radiation levels throughout the year, with a concentrated distribution pattern compared to other materials (Fig. 10f). In terms of performance, the low-cost materials AS_2.2, AS_2.3, V_1.1 and V_1.2 showed inferior performance compared to theoretical materials M5-M8, RC1, and RC2, as they absorbed a larger amount of incoming solar radiation. In this climate, the system would not be worthy of application.

Lagos and Rio de Janeiro were the representative locations of the equatorial savannah with a dry winter climate (Aw) characterized by a minimum precipitation above 60 mm in summer. The materials presented a constant behavior throughout the year in Lagos, while their behavior differed in Rio de Janeiro (Fig. 10d and e). This difference in Rio can be attributed to the fluctuations in solar radiation during the summer solstice and lower values of relative humidity, enabling higher heat losses by radiation. As a result, the radiated heat was more disperse in Rio compared to Lagos across all materials (Fig. 10f). The difference between both cities was more significant for materials RC2, M8, V_1.1, and V_1.2, being almost identical for A and M5. In Rio, material M8 (mean −37.8 $kWhm^{-2}$) evacuated heat throughout the entire year, closely followed by RC2 (mean −37.6 $kWhm^{-2}$ that was able to do so from March to November) and VS_1.1 (-38.3 $kWhm^{-2}$ from May to September) that could evacuate heat when solar radiation was low. Considering the solar heat gains and the convective heat gains and losses, the system could operate and evacuate heat in Rio but not in Lagos (Fig. 10g). In Rio, all the materials except for aluminum and those based on aluminum (AS_2.2 and AS_2.3) succeeded in evacuating heat.

3.2. Arid zone climates (B)

The hot steppe (Bsh) climate is characterized by low precipitation and annual mean near-surface temperature above 18 °C. This climate's representative cities are Monterrey and Phoenix. Despite being classified under the same climate, Monterrey had higher relative humidity than Phoenix and lower mean ambient temperatures due to lower solar radiation. Consequently, the materials exhibited very distinct behavior (Fig. 11a and b). In both cities, M8 demonstrated the best performance (59.9 $kWhm^{-2}$ (MTY) and −88 $kWhm^{-2}$ (PHX)) as it reflected all incoming radiation and could emit radiation in several wavelengths, followed closely by RC2 and VS_1.1, which evacuated heat from September to May in Monterrey and from October to May in Phoenix. As seen in Fig. 11f, the radiated heat was more disperse in Phoenix than in Monterrey for all materials. The difference between both cities was more significant in RC2, M8, and V_1.1, being identical for A. The material that radiated the most heat in both locations during more extended

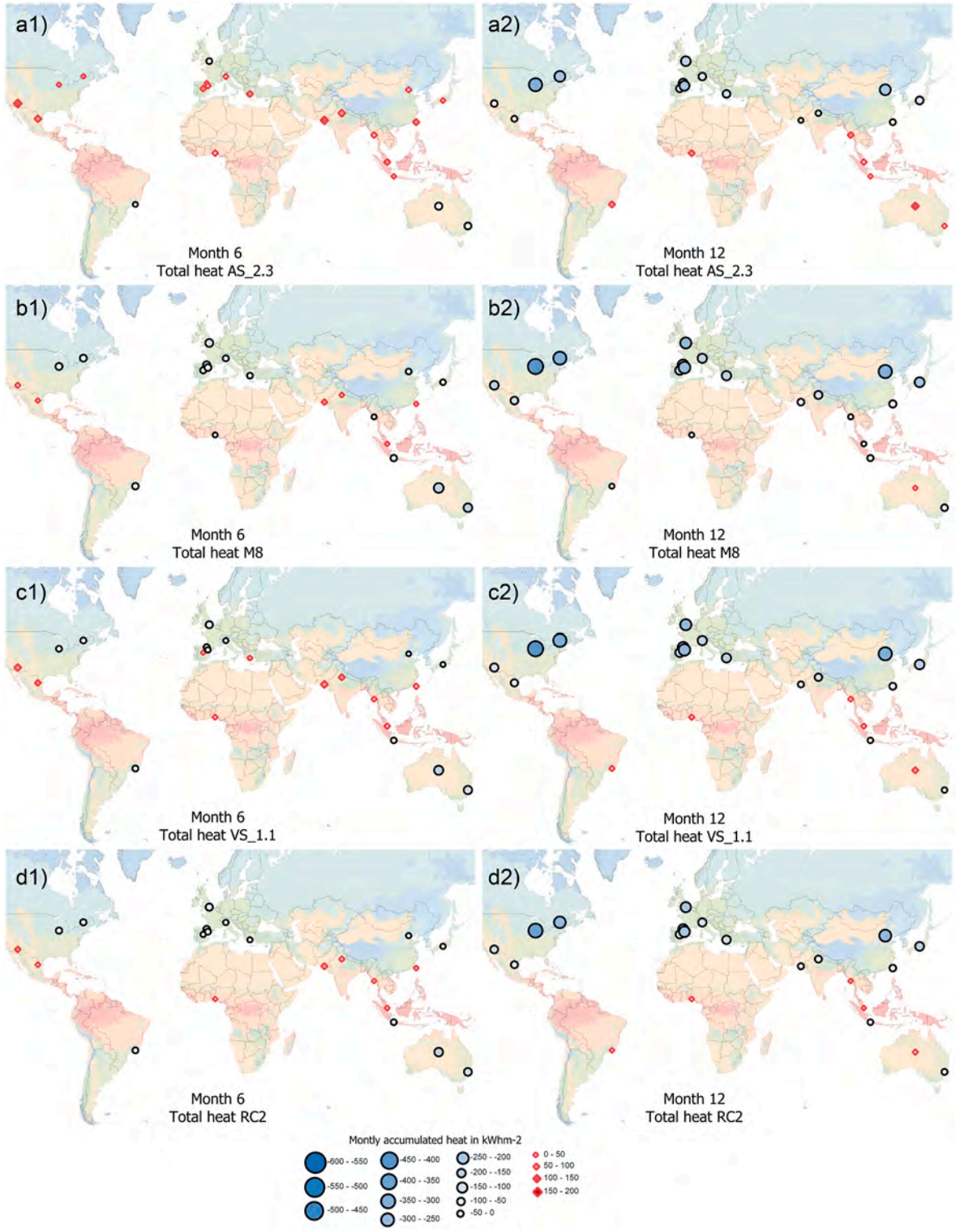

Fig. 5. Monthly accumulated heat in KWhm-2 for a1) AS_2.3 in June a2) AS_2.3 in December, b1) M8 in June, b2) M8 in December, c1) VS_1.1 in June and c2) VS_1.1 in December.

period was material V_1.1 (Fig. 11f); however, other factors counteracted the overall balance, as seen in Fig. 11g, where RC2 and M8 had slightly better behavior than V_1.1 and V_1.2. The system stored higher amounts of energy during the summer months in Phoenix due to the higher temperatures and global radiation. Nevertheless, the system was able to dissipate more heat during the winter months, which can be attributed to the lower relative humidity levels in Phoenix.

The cold steppe (BSk) climate is characterized by low precipitation and annual mean near-surface below 18 °C. This climate's representative selected city is Zaragoza. The materials presented a distinct behavior (Fig. 11c), during the winter and summer months. Materials RC2, M8, were capable of cooling throughout the entire year (Fig. 11g), while VS_1.1 was able to do so except in July where it experienced a heat gain of 5.5 $kWhm^{-2}$. This can be attributed to VS_1.1's higher absorption of energy in

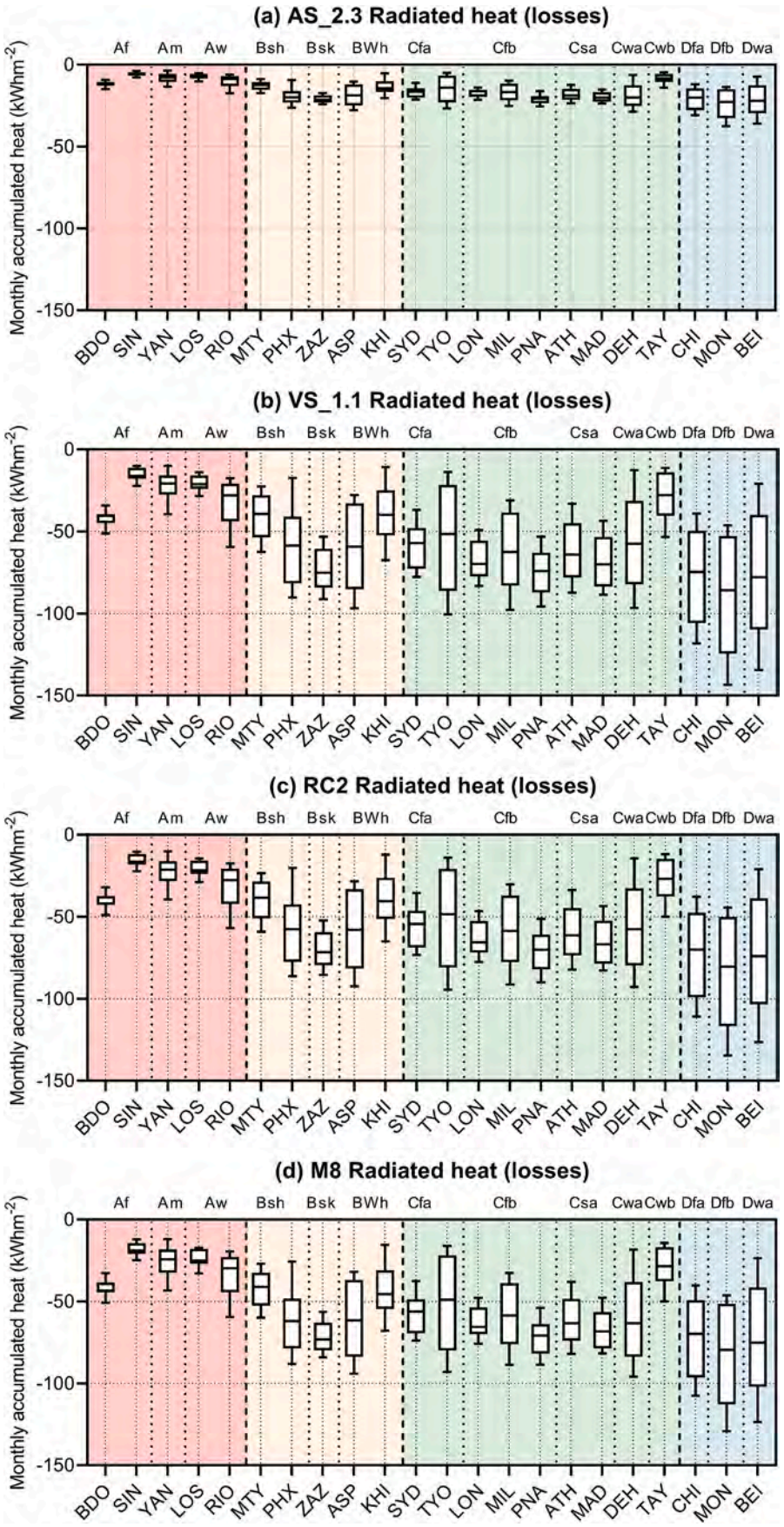

Fig. 6. Boxplots of monthly accumulated radiative heat losses by material: (a) AS_2.3, (b) VS_1.1, (c) RC2 and (d) M8 in the 22 selected cities.

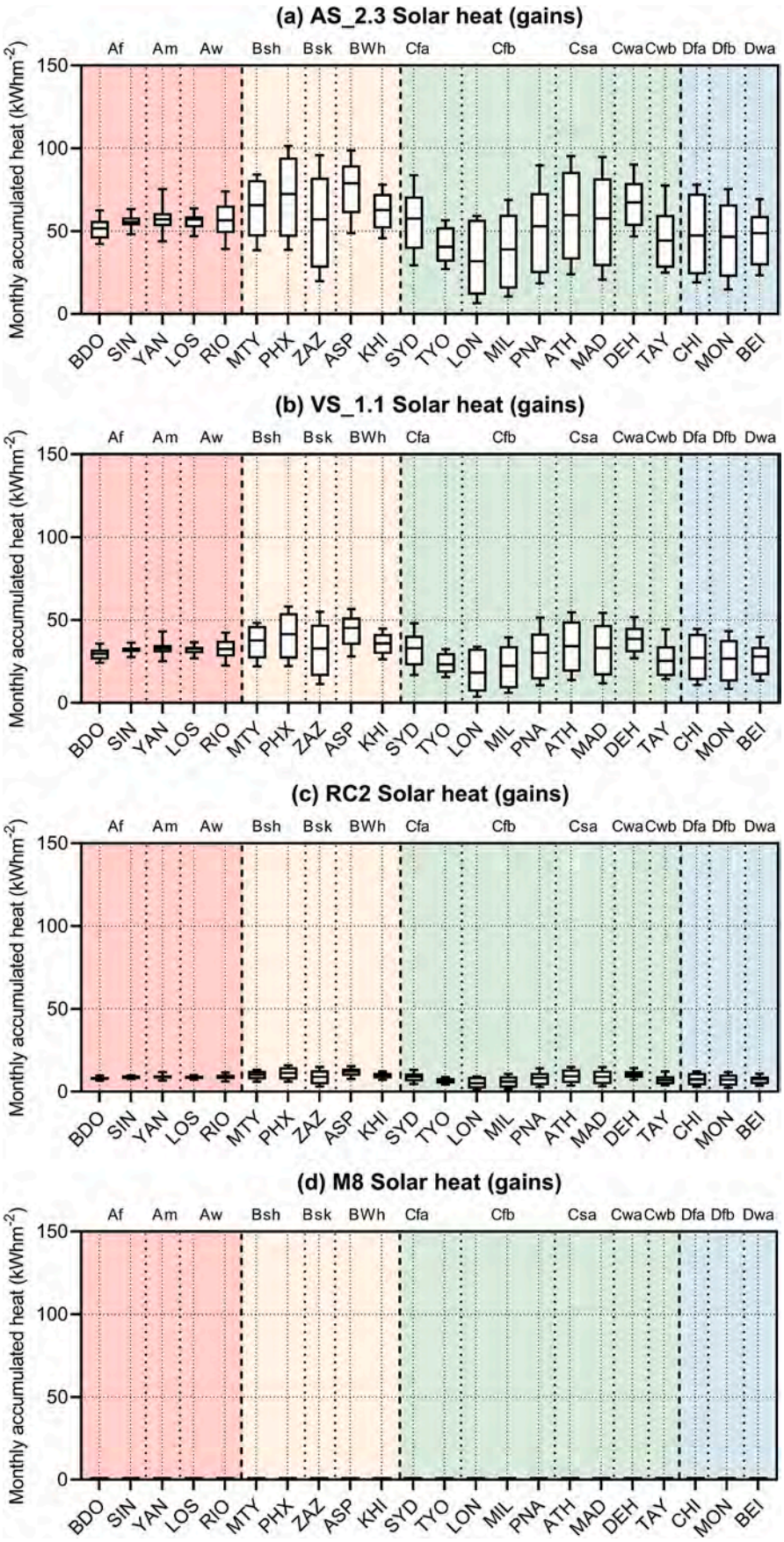

Fig. 7. Boxplots of monthly accumulated solar heat gains by material: (a) AS_2.3, (b) VS_1.1, (c) RC2 and (d) M8 in the 22 selected cities.

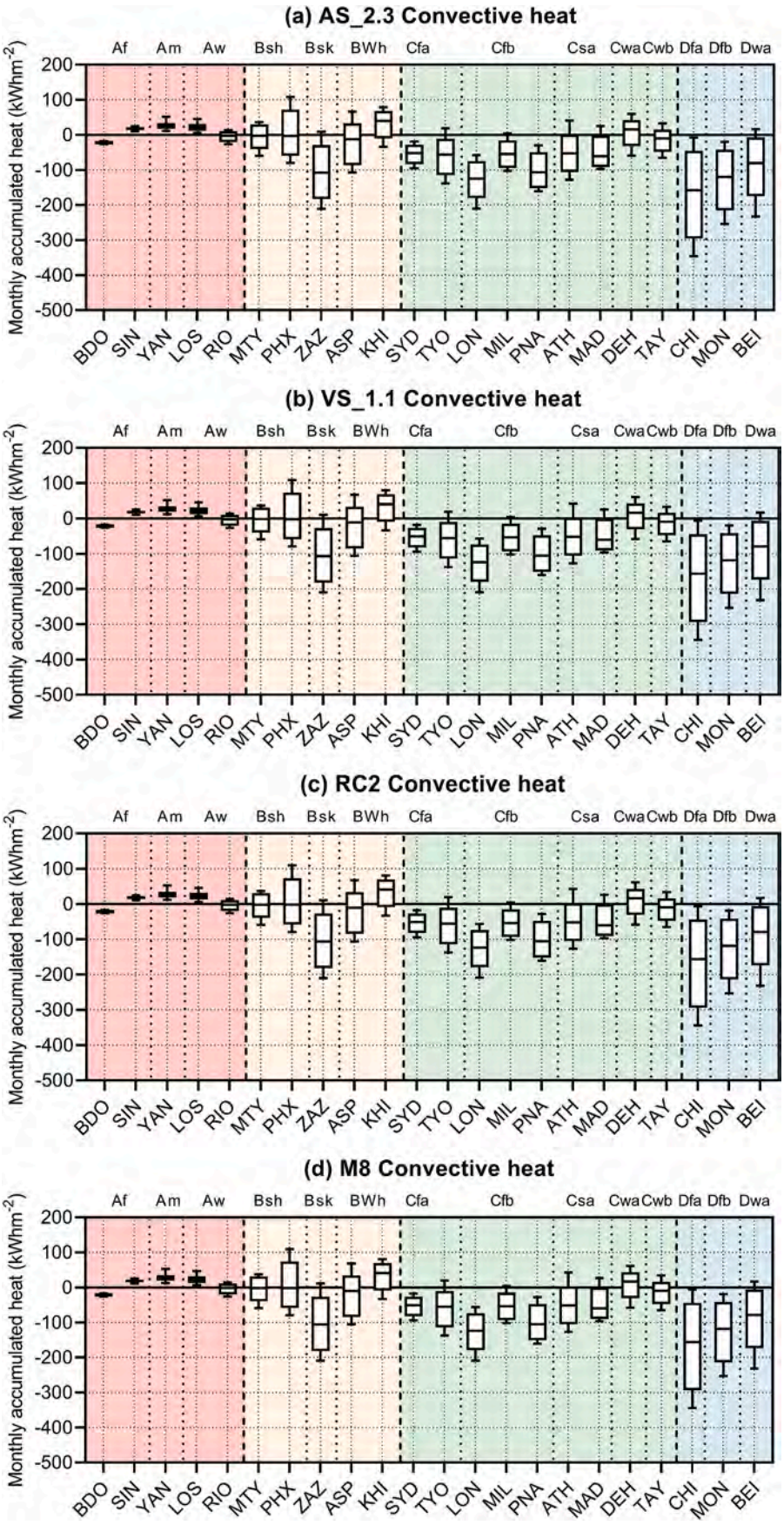

Fig. 8. Boxplots of monthly accumulated convection heat gains or losses by material: (a) AS_2.3, (b) VS_1.1, (c) RC2 and (d) M8 in the 22 selected cities.

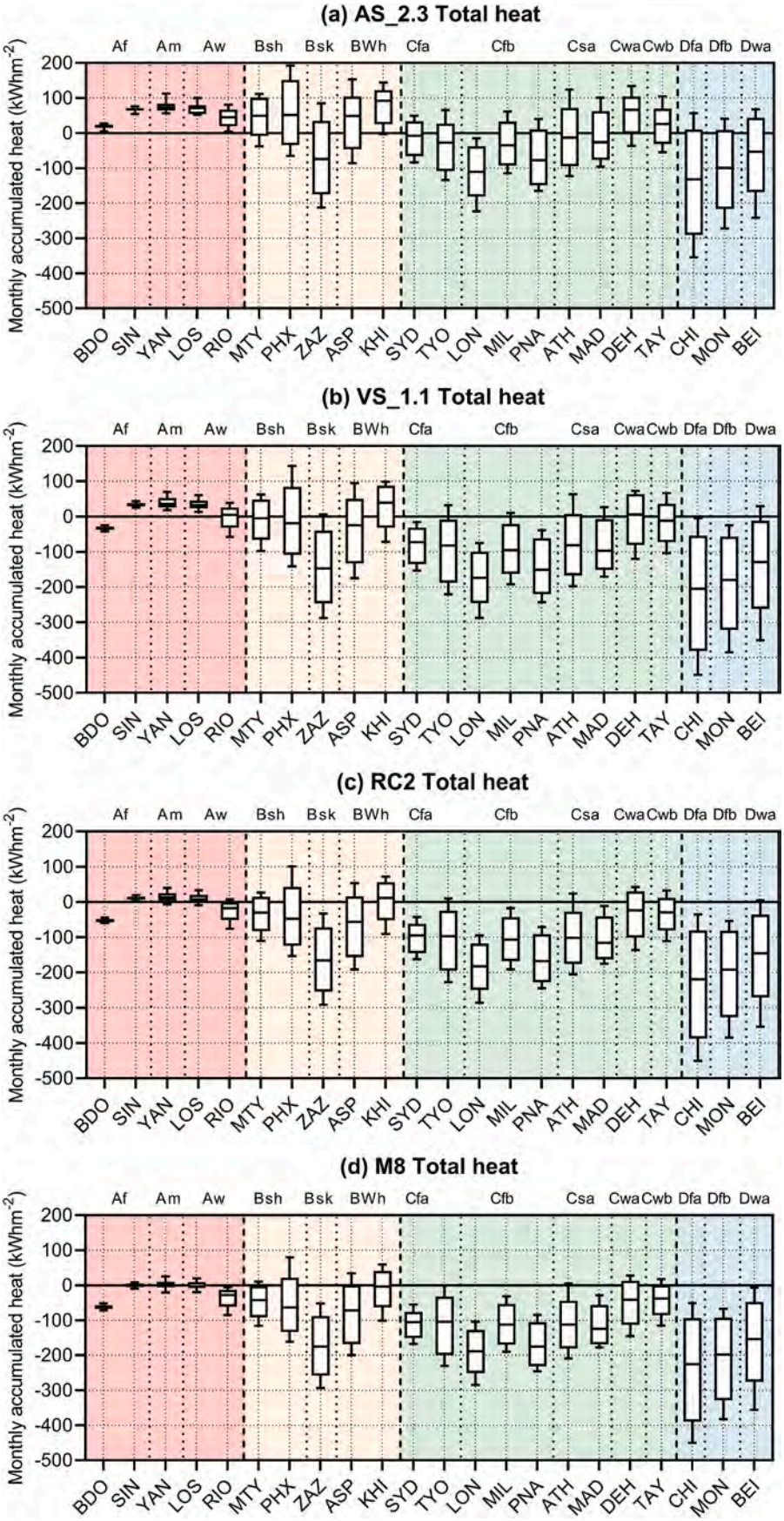

Fig. 9. Boxplots of monthly accumulated total heat balance by material: (a) AS_2.3, (b) VS_1.1, (c) RC2 and (d) M8 in the 22 selected cities.

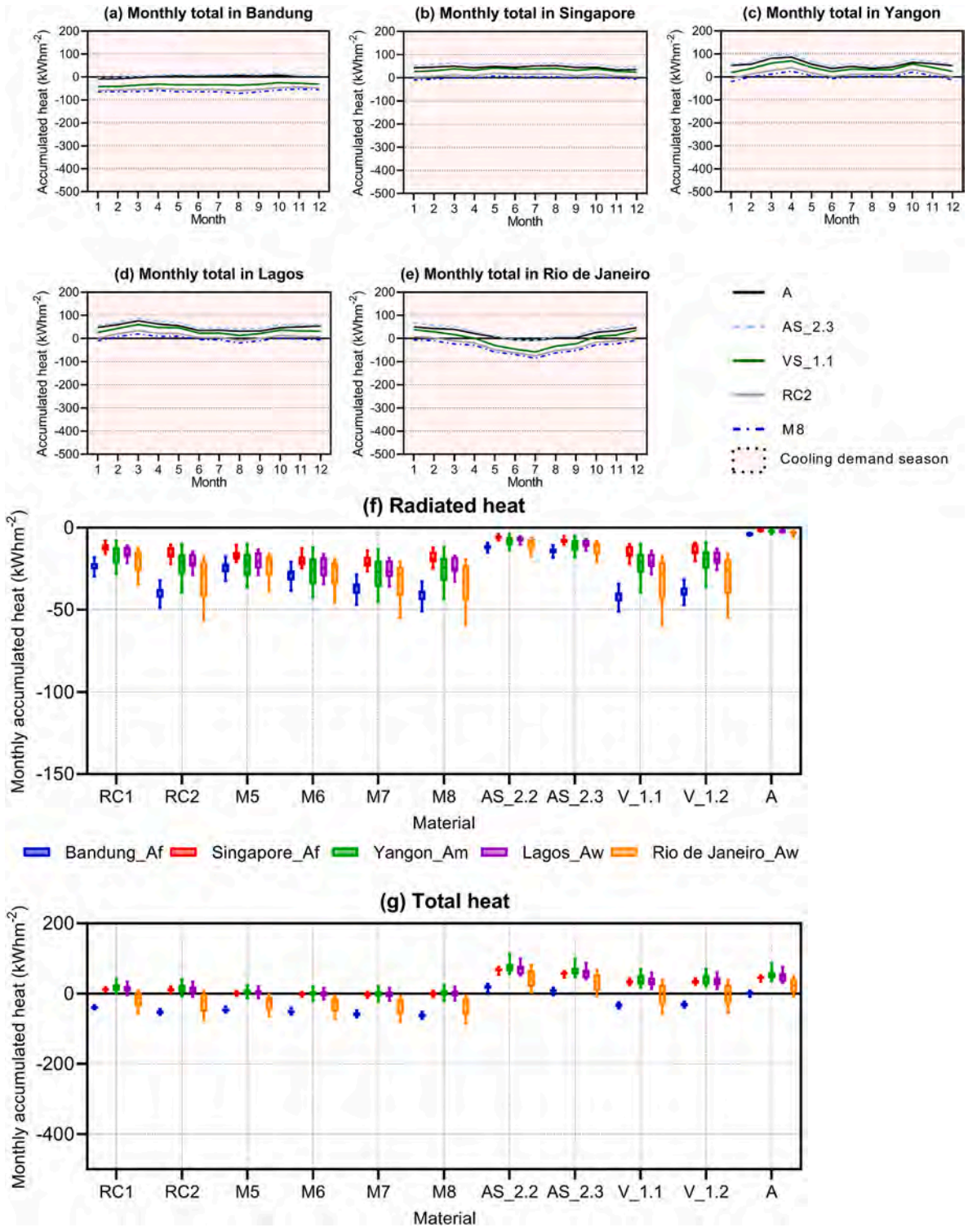

Fig. 10. A climate results. Total heat accumulated per month in: (a) Bandung, (b) Singapore, (c) Yangon, (d) Lagos, and (e) Rio de Janeiro for materials A, AS_2.3, VS_1.1, RC2 and M8; (f) monthly accumulated radiated heat variation; and (g) monthly accumulated total heat variation in the previous cities for the eleven materials.

the visible wavelengths compared to other materials. Fig. 11f illustrates the radiated heat throughout the year for the eleven materials. AS_2.2, AS_2.3, and A radiated had a stable yearly distribution, with a concentrated boxplot distribution. This is a result of their lower emissivity values infrared wavelengths. Despite Zaragoza having higher relative humidity values, the lower ambient temperatures throughout the year allowed the system to perform better than in Phoenix.

The dessert with a cold (BWh) climate is characterized by low precipitation and annual mean near-surface above 18 °C. Two cities were studied, Alice Springs, and Karachi. Karachi exhibited higher relative humidity than Alice Springs along with lower mean ambient temperatures. In both cities, the theoretical material M8 demonstrated the best behavior, evacuating an average heat of −113 kWhm^{-2} (ASP) and −56 kWhm^{-2} (KHI); closely followed by RC2, -100 kWhm$^{-2,}$ and -53

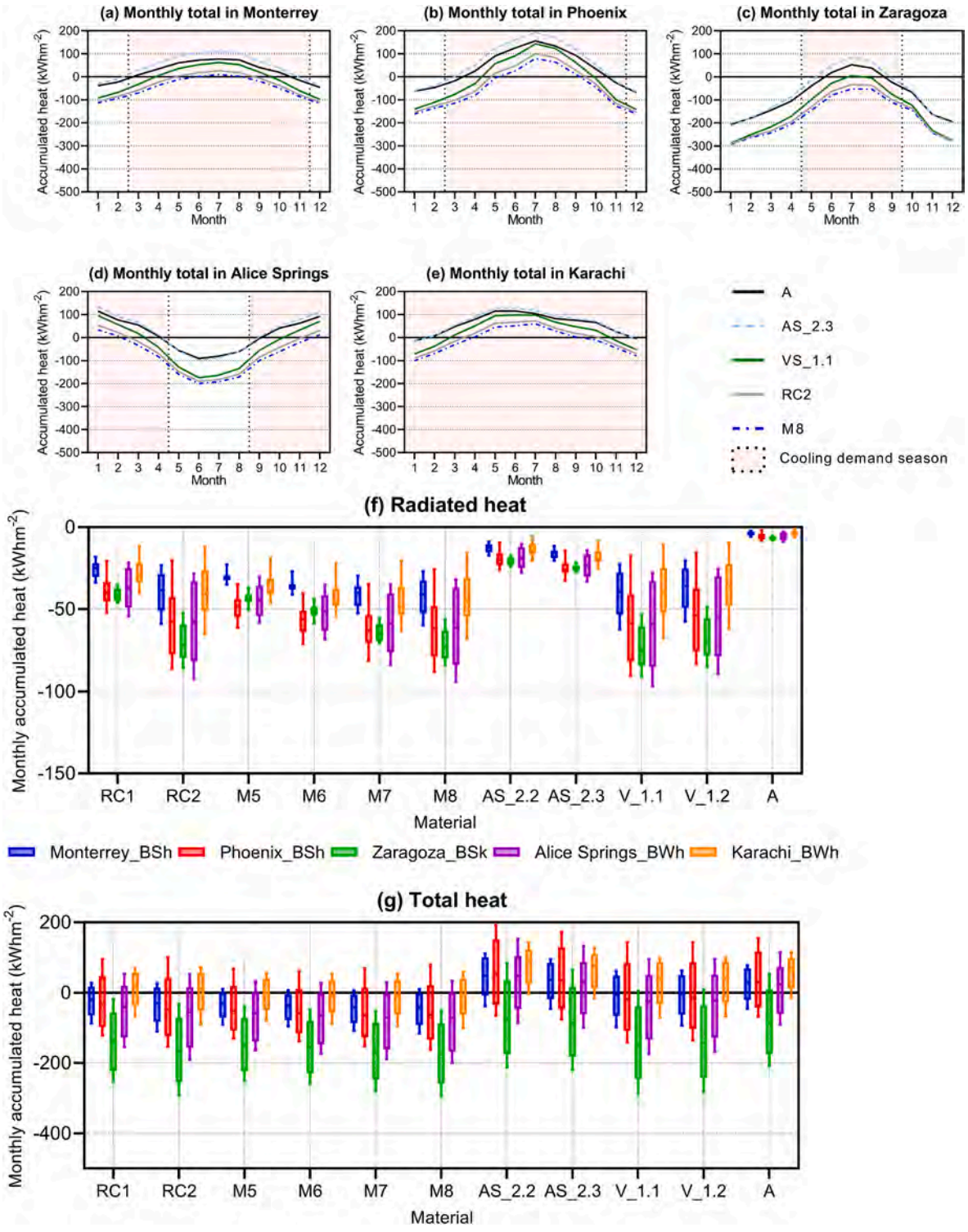

Fig. 11. B climate results. Total heat accumulated per month in: (a) Monterrey, (b) Phoenix, (c) Zaragoza, (d) Alice Springs, and (e) Karachi for materials A, AS_2.3, VS_1.1, RC2 and M8; (f) monthly accumulated radiated heat variation; and (g) monthly accumulated total heat variation in the previous cities for the eleven materials.

kWhm^{-2} and VS_1.1, −100 kWhm^{-2} and -48 kWhm^{-2}. The materials were able to evacuate almost double the yearly average heat in Alice Spring compared to Karachi. This can be attributed to the lower relative humidity levels and lower ambient temperatures during the winter months in Alice Springs. As seen in Fig. 11f, the amount of radiated heat was more disperse in Alice Springs due to the distinct incoming radiation compared to Karachi across all materials. The difference between the two cities was more significant for materials RC2, M8, V_1.1, and V_1.2, while it was identical for A, which had negligible longwave emissivity values. The material that radiated more heat in both cities over a larger number of months was V_1.1 (Fig. 11f). However, solar heat gains by material V_1.1 counteracted the total balance as depicted in Fig. 11g, where RC2 and M8 exhibited slightly better behavior compared to V_1.1 and V_1.2. This is because RC2 and M8 did not absorb as much solar

radiation as V_1.1 which contributed to their improved overall performance.

3.3. Warm temperate zone (C)

The warm temperate climate, fully humid and hot summer (Cfa) climate is characterized by the warmest month's mean temperature above 18 °C. This climate's representative cities are Sydney and Tokyo. In Sydney, materials VS_1.1, RC2, and M8 demonstrated effective heat evacuation, maintaining values below −55 kWhm^{-2} for all months (Fig. 12a), with peak evacuation reaching up to −170 kWhm^{-2}. In contrast, in Tokyo, those materials accumulated heat (Fig. 12b) from June to August. As seen in (Fig. 12f), the radiated heat was more significant in Tokyo (maximum of −93 kWhm^{-2}) than in Sydney

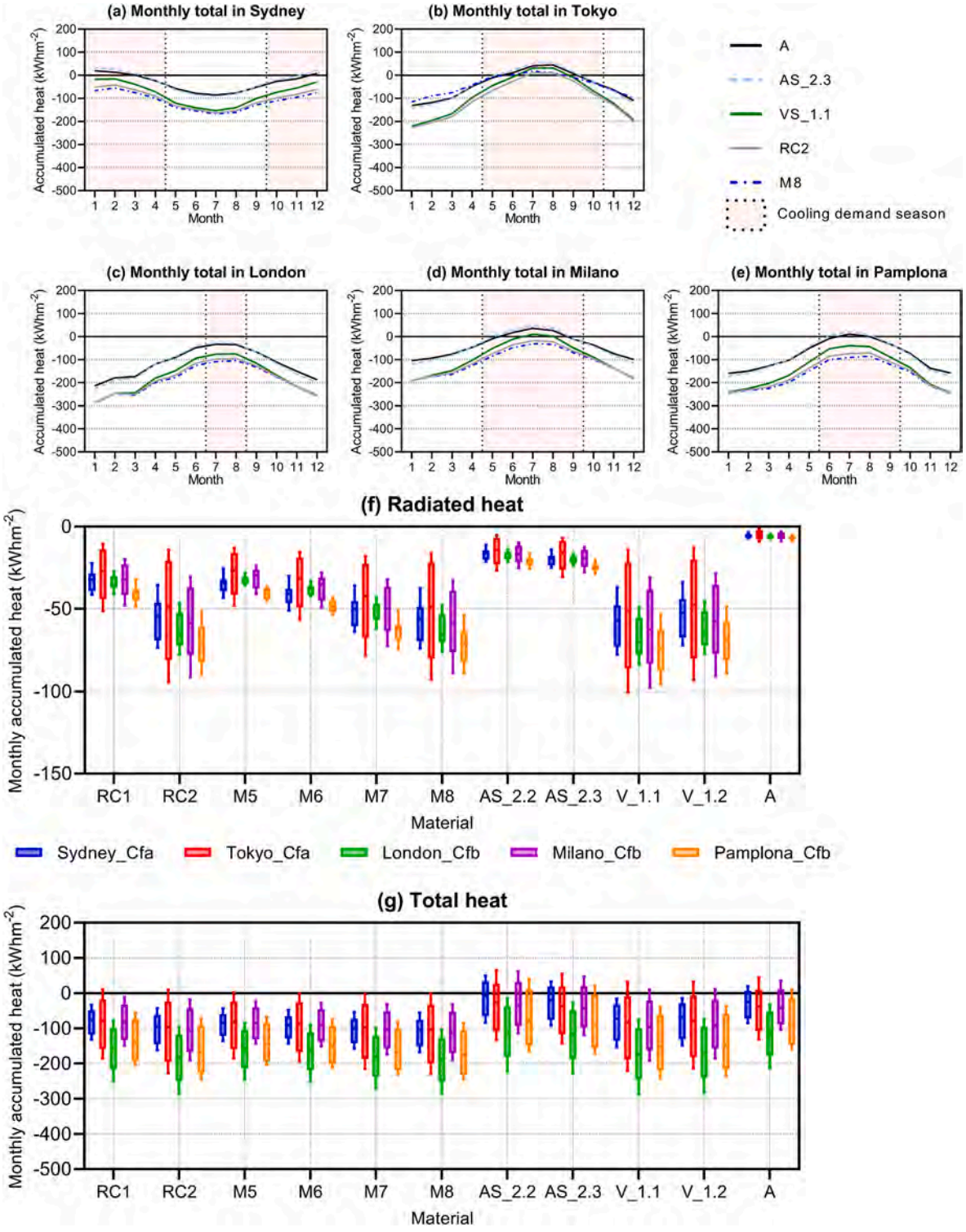

Fig. 12. Cfa and Cfb climate results. Total heat accumulated per month in: (a) Sydney, (b) Tokyo, (c) London, (d) Milano, and (e) Pamplona for materials A, AS_2.3, VS_1.1, RC2 and M8; (f) monthly accumulated radiated heat variation; and (g) monthly accumulated total heat variation in the previous cities for the eleven materials.

(maximum of −77 kWhm^{-2}) for all materials. Materials with broader the emissivity across their band exhibited greater radiation (Fig. 12f). Fig. 12g indicates that, in Sydney, all materials, except AS_2.2, AS_2.3, and A, exhibited cooling throughout the year. However, in Tokyo, as a result of the higher ambient temperatures some materials experienced greater heat gains at certain points, surpassing zero, making its application less feasible.

The warm temperate climate, fully humid with cool summer and cold winter (Cfb) representative cities are London, Milano, and Pamplona. The behavior of materials varied distinctly between winter and summer months (Fig. 12c, d, and e). In London, all materials effectively evacuated heat (Fig. 12g) throughout the year. In Milan and Pamplona, both M8 and RC2 cool down throughout the entire year, and in Pamplona V_1.1 also exhibited the same behavior. However, materials A and

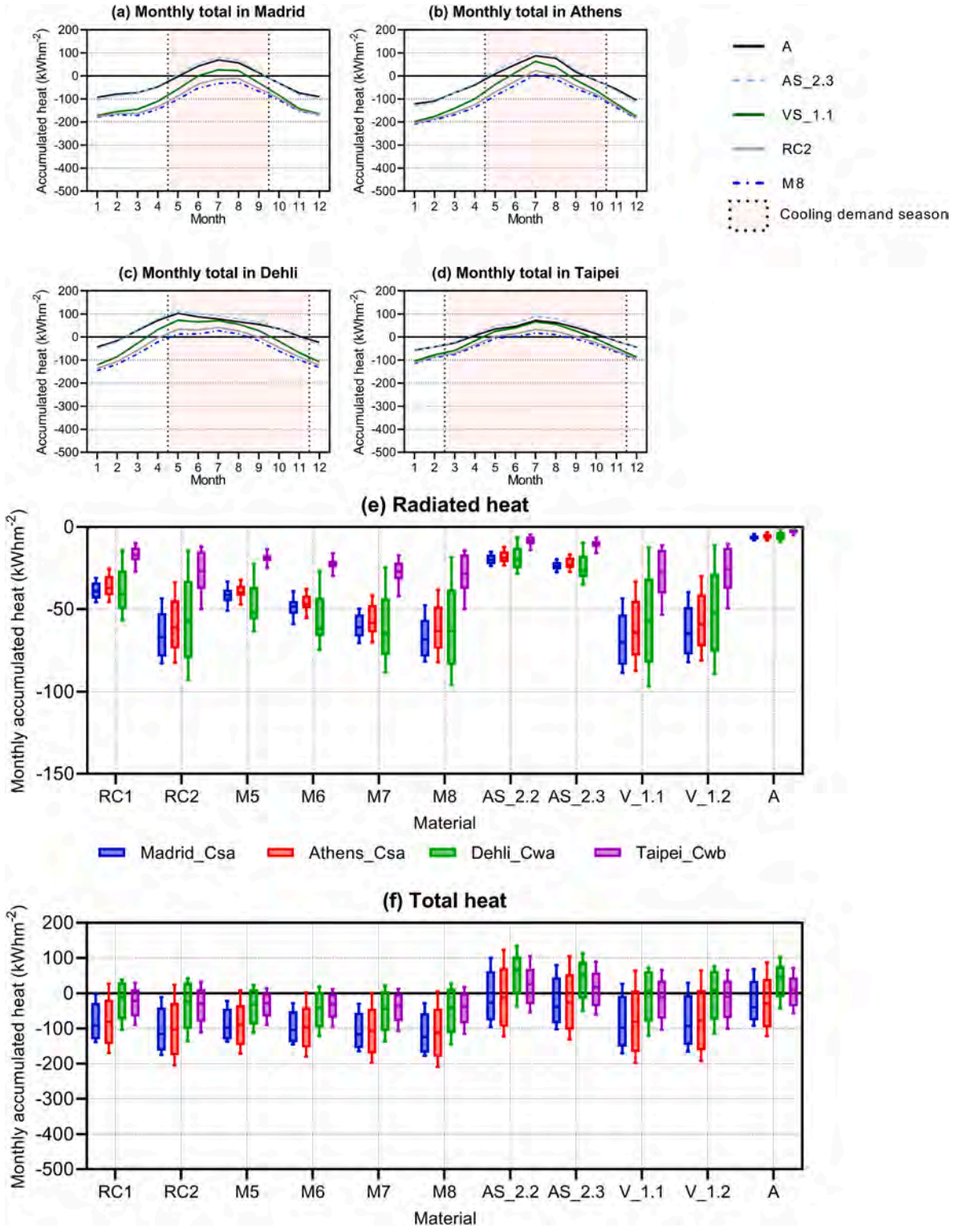

Fig. 13. Csa, Cwa and Cwb climate results. Total heat accumulated per month in: (a) Madrid, (b) Athens, (c) Delhi, and (d) Taipei for A, AS_2.3, VS_1.1, RC2 and M8; (e) monthly accumulated radiated heat variation; and (f) monthly accumulated total heat variation in the previous cities for the eleven materials.

AS_2.3 experienced heating in several months, with the accumulated heat gains being more prominent in Milan, reaching 68 kWhm^{-2} in July. As seen in Fig. 12f, the radiated heat was similar among the three cities for all materials. However, each material displayed a distinct radiative potential depending on the month, except for AS_2.2, AS_2.3, and A, which exhibited nearly constant radiative potential. The total heat was negative for most materials and in all locations, leading to substantial heat losses. In general, the materials exhibited better performance in Pamplona compared to Milan. This can be attributed to Pamplona having higher solar radiation, which does not significantly impact materials with high solar reflectivity. However, it is important to note that the higher relative humidity in Pamplona hinders longwave radiation during the summer months.

The warm temperate climate with dry, hot summer (Csa) climate is characterized by a mean temperature above 18 °C in the warmest month. The representative cities for this climate are Athens and Madrid. Fig. 13a and b, illustrate the winter-summer behavior of the materials, which were nearly identical in both locations. In Madrid, RC2 and M8 materials demonstrated year-round effective heat evacuation (Fig. 13f). A similar pattern was observed in Athens, except in July, explained by Athens' higher relative humidity in general, particularly in summer and slightly higher radiation around the summer solstice. Due to the very similar climates, the radiated heat values were comparable between the two cities. In Athens, RC2, M8, and V_1.1 achieved −82.2 kWhm^{-2}, -82 kWhm^{-2}, -87.3 kWhm$^{-2,}$ while in Madrid, the values were −82.8 kWhm^{-2}, -81.7 kWhm^{-2} and -88.4 kWhm^{-2}. During the summer period, materials performed worse in Athens, even though the radiated heat was similar in both cities for all materials (Fig. 13e). Materials V_1.1; A and AS_2.3 heated up some months in Athens, reaching up to 104 kWhm^{-2} in July. This can be explained by slightly higher solar and convective heat gains.

The warm temperate climate with dry winter and hot summer (Cwa) climate representative city is Delhi. The materials exhibited different summer-winter behavior, as seen in Fig. 13c. In Delhi, none of the materials could evacuate heat from May to August. Nevertheless, materials M8 and RC2 demonstrated potential as viable solutions for the spring and autumn months, as they exhibited heat evacuation capabilities during those periods (monthly average −83 kWhm^{-2} and -69 kWhm^{-2}), as shown in Fig. 13c. Furthermore, the radiated heat was more significant for these materials as well, reaching up to 95 kWhm^{-2} and 92 kWhm^{-2}, respectively (Fig. 13e). All the materials could evacuate heat in certain months, considering all heat transfer mechanisms as seen in Fig. 13f. In general, due to the prevailing high temperatures and relative humidity levels, the system exhibited increased solar gains and convective gains.

The warm temperate climate with dry cold winter and cool summer climate (Cwb) representative city is Taipei. In Taipei, materials VS_1.1, RC2, and M8 effectively evacuated heat from October to April, with average values of −57 kWhm^{-2}, -68 kWhm^{-2}, -74 kWhm^{-2}, respectively (Fig. 13d). As shown in Fig. 13e, the radiated heat was more pronounced for these three materials. Materials with broader emissive band such as RC2, M8, VS_1.1 and VS_1.2, exhibited great radiative power (Fig. 13e). However, the high relative humidity levels in Taipei hindered the radiative cooling effect with outer space, resulting in lower radiated heat compared to that observed in Delhi.

3.4. Snow zone climates (D)

The snow climate, fully humid, and hot summer climate (Dfa) representative city is Chicago. The materials exhibited significant behavior variation throughout the year as depicted in Fig. 14a. In Chicago, materials VS_1.1, RC2, and M8 could effectively evacuate heat in all the months (Fig. 14a). Additionally, as shown in Fig. 14d, these materials namely RC2 (av. −73 kWhm^{-2}), M8 (av.-72 kWhm^{-2}), V_1.1 (av. −77 kWhm^{-2}) and V_1.2 (av. −72 kWhm^{-2}), displayed higher levels of radiated heat. The total heat gains of the eleven materials showed a great cooling potential, particularly during winter months, attributable to low ambient temperatures. However, as the materials were theoretically part of an active system, they could be switched off. Consequently, all materials except AS_2.2, AS_2.3, and A, demonstrated cooling trends throughout entire year, facilitated by the combination of low ambient temperatures and reduced incoming solar radiation (Fig. 14e).

The snow climate, fully humid and warm summer climate (Dfb), selected representative city is Montréal. It should be noted that the materials presented a similar behavior to that observed in Chicago (Dfa). The materials displayed significant variation in behavior throughout the year (Fig. 14b) due to the contrasting summer-winter climatic conditions. In Montréal, materials VS_1.1, RC2, and M8 effectively evacuated heat during all months (Fig. 14b), with average values of −88 kWhm^{-2}, -83 kWhm$^{-2,}$ and -82 kWhm^{-2}, respectively. As seen in Fig. 14d, these materials also exhibited higher levels of radiated heat. The total heat gains for the eleven materials in (Fig. 14e) demonstrated a remarkable cooling potential the highest among all the studied locations, particularly during winter. With the exception of AS_2.2, AS_2.3, and A, all materials cooled down throughout the year. This exceptional performance has to do with low ambient temperatures and radiation found in this location.

The snow climate with dry winter and hot summer climate (Dwa) representative city is Beijing. The materials showed very similar behavior in this climate than in the previous two climates (Dfa and Dfb); however, there were slight differences. Despite having a higher radiative potential and considering all heat transfer mechanisms, the materials performed slightly less effectively in this climate. In Beijing materials, RC2 and M8 could effectively evacuate heat throughout all months (Fig. 14c). This can be explained by the fact that Beijing experiences slightly higher mean ambient temperatures than the other cities, which result in higher convective heat gains in this location. Fig. 14d demonstrates that these materials had higher levels of radiated heat, particularly those with a broadband emissivity such as RC2, M8, V_1.1, and V_1.2. The points above zero showed heat accumulations in some months. Therefore, it is advisable to switch off the system (Fig. 14e).

To summarize the findings, the ability to radiate heat is influenced by the emissivity properties of the material. Higher emissivity allows for greater heat evacuation. For example, aluminum (A) showed the least radiated heat losses, while VS_1.1 exhibited the highest radiated heat losses across all cities (Fig. 7a), with the lowest value being −9.3 kWhm^{-2} in Yangon (Am) and −143 kWhm^{-2} in Montreal (Dfb). Solar heat gains, on the other hand, depend on the materials' reflectivity properties mostly in the solar visible wavelength range (0.3–1 μm). The theoretical material M8 demonstrating perfect solar reflectivity, resulting in no solar gains (Fig. 8b) in any of the cities. On the contrary, materials with the low-cost emissive coating (VS and AS) had higher solar heat gains since the emissive layer partially reduces the materials' solar reflectivity (see Figs. 6b and 7b). RC2 exhibited better solar behavior than V_1.1, despite having slightly worse emissivity; leading to a better overall balance for RC2.

Solar heat gains were higher in cities with greater incident solar radiation, such as Phoenix, Alice Springs, Delhi, Athens, and Madrid. Materials VS_1.1 and RC2 displayed similar behavior across all those climates; with greater radiated cooling power observed in locations with lower mean ambient temperatures, as ambient temperature is a determinant factor [44]. The total accumulated heat is a combination of convective heat gains or losses, radiative losses, and solar gains. Since convection for the materials was the same within the same location but varied among the cities, as surface was stable at 25 °C, the materials with nearly ideal reflectivity and higher infrared emissivity presented greater heat losses. As a summary, Table 1 shows the total heat exchanged for materials AS_2.3, V_1.1, RC2 and M8, for the months of June and December in all the cities under study.

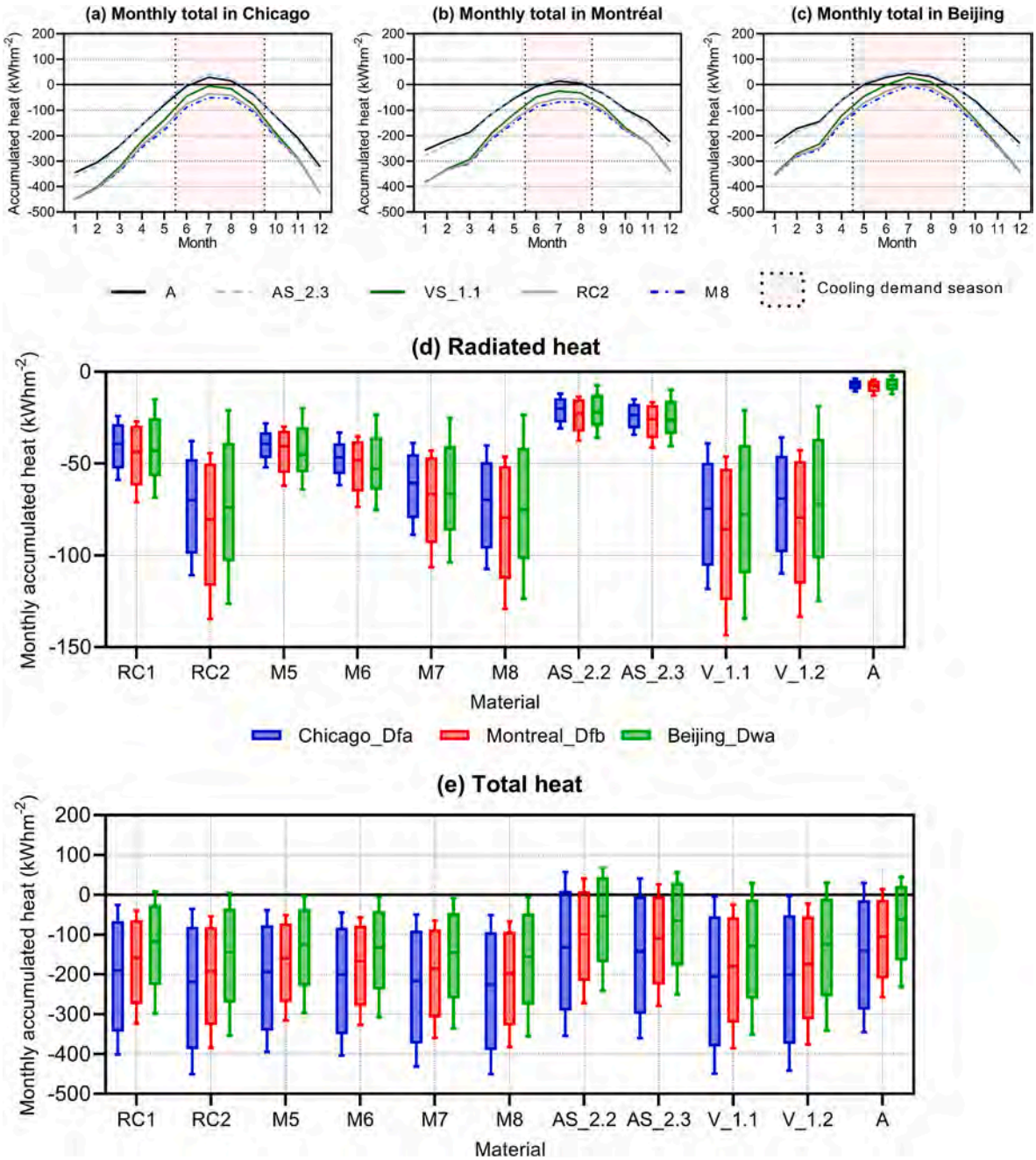

Fig. 14. D climate results. Total heat accumulated per month in: (a) Chicago, (b) Montreal, and (c) Beijing, for A, AS_2.3, VS_1.1, RC2 and M8; (d) monthly accumulated radiated heat variation; and (e) monthly accumulated total heat variation in the previous cities for the eleven materials.

4. Discussion and conclusions

This research is the first to simulate and calculate the potential of different existing materials under the same climatic conditions. Up until now, the behavior and thermal response of the daytime radiative cooling materials in the literature could not be directly compared. Moreover, some experiments referred to temperature at which the samples achieved thermal equilibrium while others supplied heating power to the samples to maintain the samples at ambient temperature. Besides, the location and weather conditions of the experiments vary a lot, therefore, making it impossible to compare the materials' behavior.

To solve this gap, the present research has made it possible to compare under the same weather conditions the behavior of different radiative cooling materials the most prevalent climates across the world. The study conducted a simulation of an active application involving the placement of radiative cooling materials on a highly conductive surface. The system assumed no insulation and simulated a scenario similar to an active system with a fluid or constant-temperature heat source beneath the surface. The model calculated the hourly heat gains or losses to determine the cooling potential. The temperature below the material was set at 25 °C, and the external heat transfer coefficient considered factors like surface temperature, ambient air temperature, and wind speed. The chosen temperature and heat transfer coefficient aimed to reflect typical comfort conditions inside buildings during the cooling period and resemble forced convection of a liquid flowing through a pipe in an active system. However, for practical implementation, it would be necessary to establish a threshold for the total heat, below which it would not be deemed worthwhile to implement.

Although the results presented refer to the selected cities, it is possible to draw general conclusions since multiple cities were chosen to

Table 1
Total heat exchanged ($kWhm^{-2}$) between the surface and the environment for the different materials in two months June and December.

Climate	Abbr	City (Country)	AS_2.3		V_1.1		RC2		M8	
			Jun.	Dec.	Jun.	Dec.	Jun.	Dec.	Jun.	Dec.
Equatorial zone climates (A)										
Af	BDO	Bandung (Indonesia)	8,4	6,4	−34,8	−30,6	−54,7	−48,0	−64,4	−56,0
Af	SIN	Singapore (Singapore)	57,0	46,5	37,5	24,9	15,1	4,1	4,5	−5,9
Am	YAN	Yangon City (Myanmar)	47,2	56,3	23,2	23,6	2,0	−0,6	−8,0	−13,0
Aw	LOS	Lagos (Nigeria)	44,1	61,1	23,2	31,4	3,9	7,2	−5,3	−5,5
Aw	RIO	Rio de Janeiro (Brazil)	−5,3	63,3	−46,7	35,0	−61,0	5,7	−69,0	−7,3
Arid zone climates (B)										
BSh	MTY	Monterrey (Mexico)	88,2	−46,5	52,9	−97,6	18,2	−110,0	1,6	−116,3
BSh	PHX	Phoenix (USA)	137,3	−75,5	91,4	−141,6	47,5	−153,3	25,2	−160,2
BSk	ZAZ	Zaragoza (Spain)	30,3	−207,2	−27,3	−275,8	−62,6	−278,2	−80,0	−279,9
BWh	ASP	Alice Springs (Australia)	−99,2	110,9	−175,0	70,3	−190,6	30,3	−199,8	11,7
BWh	KHI	Karachi (Pakistan)	127,5	−5,9	98,2	−52,8	66,7	−69,8	50,8	−79,5
Warm temperate climates (C)										
Cfa	SYD	Sydney (Australia)	−85,0	22,0	−141,2	−28,9	−149,3	−60,8	−154,4	−75,7
Cfa	TYO	Tokyo (Japan)	20,3	−122,2	−7,9	−194,9	−26,7	−200,6	−35,2	−204,2
Cfb	LON	London (UK)	−41,9	−198,9	−94,1	−256,3	−115,3	−253,5	−125,3	−252,4
Cfb	MIL	Milano (Italy)	27,4	−113,4	−11,4	−182,6	−36,2	−180,7	−47,9	−179,7
Cfb	PNA	Pamplona (Spain)	3,5	−171,7	−53,1	−243,0	−85,2	−244,7	−100,2	−246,3
Csa	MAD	Madrid (Spain)	53,9	−99,9	0,4	−164,1	−35,4	−167,2	−53,0	−168,9
Csa	ATH	Athens (Greece)	64,2	−115,3	15,0	−176,4	−22,3	−181,7	−40,1	−185,4
Cwa	DEH	Delhi (India)	99,3	−33,4	65,8	−107,1	31,0	−122,7	13,1	−133,1
Cwb	TAY	Taipei (Taiwan)	61,0	−46,0	40,1	−86,5	14,4	−94,6	2,5	−99,2
Snow zone climates (D)										
Dfa	CHI	Chicago (USA)	5,7	−339,4	−45,4	−427,1	−75,1	−427,5	−89,1	−427,2
Dfb	MON	Montréal (Canada)	4,9	−244,1	−47,6	−339,2	−75,0	−337,1	−87,5	−335,0
Dwa	BEI	Beijing (China)	37,6	−248,3	−0,8	−341,5	−26,2	−343,5	−38,9	−344,3

represent these prevalent climates. Furthermore, the meteorological data utilized in this study is more realistic compared to that found in the existing literature, as it accounts for cloud cover through the cloudiness factor (0–1). Upon analyzing the total accumulated heat for all materials in equatorial climates (A climates: Af, Am, and Aw) cities such as Bandung, Singapore, Yangon, Lagos, and Rio de Janeiro, it was observed that the materials offered minimal benefits due to insignificant radiated heat losses and counteracting convective heat gains.

In arid climates (B climates: Bsh, Bsk, and BWh), Monterrey, Phoenix, Zaragoza, Alice Springs, and Karachi, the proposed system shows potential benefits. During transitional periods such as fall and spring, when cooling is required, radiative cooling systems could be employed. In Zaragoza, the active system utilizing materials RC2 and developed material V_1.1 exhibited the capability to dissipate sufficient heat for maintaining comfortable interior conditions throughout the year. However, it should be noted that the system may not be suitable for Karachi. The city's highest mean ambient temperatures coincided with the highest relative humidity values, impeding effective heat exchange and rendering the system less effective.

In cities with warm temperate climate (C climates: Cfa, Cfb, Csa, Cwa, and Cwb), the proposed system showed significant potential for summer cooling. Sydney and Tokyo are particularly suitable target locations due to their prolonged periods of cooling demands. In London, Milan, and Pamplona current cooling demands are relatively lower compared to heating demands; however, the system could still be used during periods of high cooling demand. Additionally, as temperatures continue to rise, this system becomes a great candidate for addressing the increasing heat.

Likewise, in temperate locations, active solutions should be favored over passive applications. This is because an active system would not result in heat penalties during the winter months. In temperate climates, the low-cost scalable materials (V_1.1 and V_1.2) might be of high interest. Cities with Csa climates such as Madrid or Athens are prime candidates that would greatly benefit from this type of application. However, in Cwa and Cwb climates, the system exhibited a less satisfactory performance. This behavior can be attributed to the higher relative humidity in cities like Delhi and Taipei, which hindered the effectiveness of radiative cooling exchange, especially in the latter. In snow zone climates (D climates: Dfa, Dfb, and Dwa), found in locations like Chicago, Montréal, and Beijing, the system demonstrated excellent cooling potential, especially during winter when heating is needed and not cooling. Nevertheless, it should be noted that the system could be implemented scenarios with higher cooling demands than residential housing.

To conclude, this research provided a comprehensive comparison of daytime radiative cooling materials across various of climates and global locations. The results showed the performance of several types of daytime radiative cooling materials. The simulations were conducted under the condition of a building with an interior temperature of 25 °C, which is considered comfortable during the summer months. The studied materials showed a great potential of heat evacuation. In arid climates, RC2 and M8 exhibited better performance compared to temperate climates due to their broadband emissivity. Most materials showed satisfactory behavior; making the choice of V_1.1 or V_1.2 types sufficient. Climates with higher relative humidity showed similar radiative behavior among the materials, with little difference observed. Convection played a crucial role in the overall heat loss or gains. In certain locations, such as arid locations with higher ambient temperatures, adding a convection barrier would enhance the system's applicability during the most demanding periods. In general, we can conclude that integrating broadband radiative cooling material as part of active systems would be more beneficial, especially in dry climates.

It must be noted that this research focused on the inherent properties of materials in heat evacuation across the most relevant world climates, without coupling them to any specific cooling system. Once the materials' behavior and worldwide potential have been studied, the next logical step is to study the integration of the optimal material with the most suitable active system for each location. Moreover, when coupled with a system, the refrigeration cycle location should be carefully studied, along with the optimal temperature of the fluid to maximize the benefits of any radiative cooling material. Finally, including an accumulator of refrigerated fluid could store the cooled fluid during the night, expanding the application possibilities. Future research will be conducted following this line. Building upon the knowledge of radiative cooling and advancements in material development, it is expected that new constructive norms, standards, and directives will contribute to the

realization of high-efficient buildings and near-zero energy buildings (nZEB). Passive approaches, along with optimized construction, technology, and installations, coupled with the application of daytime radiative cooling materials, have the potential to reduce cooling loads in buildings. Applying the knowledge of radiative cooling and new material developments in certain climates might positively impact energy balance, increasing user comfort. As a result, it will steer towards achieving the global target of reducing CO_2 emissions.

CRediT authorship contribution statement

Laura Carlosena: Writing – original draft, Visualization, Validation, Methodology, Investigation, Formal analysis, Conceptualization. **Álvaro Ruiz-Pardo:** Writing – review & editing, Validation, Software, Data curation. **Enrique Ángel Rodríguez-Jara:** Writing – review & editing, Validation, Software, Data curation. **Mattheos Santamouris:** Writing – review & editing, Supervision, Investigation.

Declaration of competing interest

The authors declare that they have no known competing financial interests or personal relationships that could have appeared to influence the work reported in this paper.

Data availability

Data will be made available on request.

Acknowledgement

Open access funding provided by Universidad Pública de Navarra.

Appendix A. Supplementary data

Supplementary data to this article can be found online at https://doi.org/10.1016/j.buildenv.2023.110694.

References

[1] IPCC, Global Warming of 1.5°C an IPCC Special Report on the Impacts of Global Warming of 1.5°C above Pre-industrial Levels and Related Global Greenhouse Gas Emission Pathways, in the Context of Strengthening the Global Response to the Threat of Climate Change, Sustainable Development, and Efforts to Eradicate Poverty, 2018.
[2] IEA, The Future of Cooling, Opportunities for Energy-Efficient Air Conditioning, International Energy Agency, 2018.
[3] C. de Munck, G. Pigeon, V. Masson, F. Meunier, P. Bousquet, B. Tréméac, M. Merchat, P. Poeuf, C. Marchadier, How much can air conditioning increase air temperatures for a city like Paris, France? Int. J. Climatol. 33 (2013) 210–227, https://doi.org/10.1002/joc.3415.
[4] V. Viguie, A. Lemonsu, S. Hallegatte, A.-L. Beaulant, C. Marchadier, V. Masson, G. Pigeon, J.-L. Salagnac, Early adaptation to heat waves and future reduction of air-conditioning energy use in Paris, Environ. Res. Lett. (2020), https://doi.org/10.1088/1748-9326/ab6a24.
[5] Y. Wang, Y. Li, S.D. Sabatino, A. Martilli, P.W. Chan, Effects of anthropogenic heat due to air-conditioning systems on an extreme high temperature event in Hong Kong, Environ. Res. Lett. 13 (2018), 034015, https://doi.org/10.1088/1748-9326/aaa848.
[6] S. Buranyi, The Air Conditioning Trap: How Cold Air Is Heating the World, The Guardian, 2019. https://www.theguardian.com/environment/2019/aug/29/the-air-conditioning-trap-how-cold-air-is-heating-the-world. (Accessed 19 November 2019).
[7] C. Yin, M. Yuan, Y. Lu, Y. Huang, Y. Liu, Effects of urban form on the urban heat island effect based on spatial regression model, Sci. Total Environ. 634 (2018) 696–704, https://doi.org/10.1016/j.scitotenv.2018.03.350.
[8] M. Santamouris, A. Synnefa, T. Karlessi, Using advanced cool materials in the urban built environment to mitigate heat islands and improve thermal comfort conditions, Sol. Energy 85 (2011) 3085–3102, https://doi.org/10.1016/j.solener.2010.12.023.
[9] M. Santamouris, Recent progress on urban overheating and heat island research. Integrated assessment of the energy, environmental, vulnerability and health impact. Synergies with the global climate change, Energy Build. 207 (2020), 109482, https://doi.org/10.1016/j.enbuild.2019.109482.
[10] E. Vardoulakis, D. Karamanis, A. Fotiadi, G. Mihalakakou, The urban heat island effect in a small Mediterranean city of high summer temperatures and cooling energy demands, Sol. Energy 94 (2013) 128–144, https://doi.org/10.1016/j.solener.2013.04.016.
[11] M. Santamouris, Analyzing the heat island magnitude and characteristics in one hundred Asian and Australian cities and regions, Sci. Total Environ. (2015) 582–598, https://doi.org/10.1016/j.scitotenv.2015.01.060, 512–513.
[12] M. Santamouris, Innovating to zero the building sector in Europe: minimising the energy consumption, eradication of the energy poverty and mitigating the local climate change, Sol. Energy 128 (2016) 61–94, https://doi.org/10.1016/j.solener.2016.01.021.
[13] M. Santamouris, D. Kolokotsa, On the impact of urban overheating and extreme climatic conditions on housing, energy, comfort and environmental quality of vulnerable population in Europe, Energy Build. 98 (2015) 125–133, https://doi.org/10.1016/j.enbuild.2014.08.050.
[14] G. Brooke Anderson, M.L. Bell, Heat waves in the United States: mortality risk during heat waves and effect modification by heat wave characteristics in 43 U.S. Communities, Environ. Health Perspect. 119 (2011) 210–218, https://doi.org/10.1289/ehp.1002313.
[15] L. Harlan Sharon, H. Declet-Barreto Juan, L. Stefanov William, B. Petitti Diana, Neighborhood effects on heat deaths: social and environmental predictors of vulnerability in maricopa county, Arizona, Environ. Health Perspect. 121 (2013) 197–204, https://doi.org/10.1289/ehp.1104625.
[16] L. Carlosena, A. Carlosena, The trend of heat-related mortality in Spain, in: N. Aghamohammadi, M. Santamouris (Eds.), Urban Overheating Heat Mitig. Impact Health, Springer Nature, Singapore, 2022, pp. 321–341, https://doi.org/10.1007/978-981-19-4707-0_16.
[17] D. Kolokotsa, G. Giannariakis, K. Gobakis, G. Giannarakis, A. Synnefa, M. Santamouris, Cool roofs and cool pavements application in Acharnes, Greece, Sustain. Cities Soc. 37 (2018) 466–474, https://doi.org/10.1016/j.scs.2017.11.035.
[18] M. Foustalieraki, M.N. Assimakopoulos, M. Santamouris, H. Pangalou, Energy performance of a medium scale green roof system installed on a commercial building using numerical and experimental data recorded during the cold period of the year, Energy Build. 135 (2017) 33–38, https://doi.org/10.1016/j.enbuild.2016.10.056.
[19] K. Gao, M. Santamouris, J. Feng, On the efficiency of using transpiration cooling to mitigate urban heat, Climate 8 (2020) 69, https://doi.org/10.3390/cli8060069.
[20] I. Kousis, C. Fabiani, L. Gobbi, A.L. Pisello, Phosphorescent-based pavements for counteracting urban overheating – a proof of concept, Sol. Energy 202 (2020) 540–552, https://doi.org/10.1016/j.solener.2020.03.092.
[21] F. Rosso, C. Fabiani, C. Chiatti, A.L. Pisello, Cool, photoluminescent paints towards energy consumption reductions in the built environment, J. Phys. Conf. Ser. 1343 (2019), 012198, https://doi.org/10.1088/1742-6596/1343/1/012198.
[22] W. Wang, N. Fernandez, S. Katipamula, K. Alvine, Performance assessment of a photonic radiative cooling system for office buildings, Renew. Energy 118 (2018) 265–277, https://doi.org/10.1016/j.renene.2017.10.062.
[23] K. Zhang, D. Zhao, X. Yin, R. Yang, G. Tan, Energy saving and economic analysis of a new hybrid radiative cooling system for single-family houses in the USA, Appl. Energy 224 (2018) 371–381, https://doi.org/10.1016/j.apenergy.2018.04.115.
[24] L. Chen, K. Zhang, M. Ma, S. Tang, F. Li, X. Niu, Sub-ambient radiative cooling and its application in buildings, Build. Simulat. 13 (2020) 1165–1189, https://doi.org/10.1007/s12273-020-0646-x.
[25] X. Li, B. Sun, C. Sui, A. Nandi, H. Fang, Y. Peng, G. Tan, P.-C. Hsu, Integration of daytime radiative cooling and solar heating for year-round energy saving in buildings, Nat. Commun. 11 (2020) 6101, https://doi.org/10.1038/s41467-020-19790-x.
[26] A. Baniassadi, D.J. Sailor, G.A. Ban-Weiss, Potential energy and climate benefits of super-cool materials as a rooftop strategy, Urban Clim. 29 (2019), 100495, https://doi.org/10.1016/j.uclim.2019.100495.
[27] A. Khan, L. Carlosena, S. Khorat, R. Khatun, Q.-V. Doan, J. Feng, M. Santamouris, On the winter overcooling penalty of super cool photonic materials in cities, Adv. Sol. Energy 1 (2021), 100009, https://doi.org/10.1016/j.seja.2021.100009.
[28] A. Khan, L. Carlosena, J. Feng, S. Khorat, R. Khatun, Q.-V. Doan, M. Santamouris, Optically modulated passive broadband daytime radiative cooling materials can cool cities in summer and heat cities in winter, Sustainability 14 (2022) 1110, https://doi.org/10.3390/su14031110.
[29] N. Fernandez, W. Wang, K.J. Alvine, S. Katipamula, Energy Savings Potential of Radiative Cooling Technologies, Pacific Northwest National Laboratory (PNNL), 2015, https://doi.org/10.2172/1234791. Richland, WA (US).
[30] A.P. Raman, M.A. Anoma, L. Zhu, E. Rephaeli, S. Fan, Passive radiative cooling below ambient air temperature under direct sunlight, Nature 515 (2014) 540–544, https://doi.org/10.1038/nature13883.
[31] S. Vall, A. Castell, M. Medrano, Energy savings potential of a novel radiative cooling and solar thermal collection concept in buildings for various world climates, Energy Technol. 6 (2018) 2200–2209, https://doi.org/10.1002/ente.201800164.
[32] Y. Zhai, Y. Ma, S.N. David, D. Zhao, R. Lou, G. Tan, R. Yang, X. Yin, Scalable-manufactured randomized glass-polymer hybrid metamaterial for daytime radiative cooling, Science 355 (2017) 1062–1066, https://doi.org/10.1126/science.aai7899.
[33] C. Liu, Y. Wu, B. Wang, C.Y. Zhao, H. Bao, Effect of atmospheric water vapor on radiative cooling performance of different surfaces, Sol. Energy 183 (2019) 218–225, https://doi.org/10.1016/j.solener.2019.03.011.
[34] L. Carlosena, Á. Ruiz-Pardo, J. Feng, O. Irulegi, R.J. Hernández-Minguillón, M. Santamouris, On the energy potential of daytime radiative cooling for urban

heat island mitigation, Sol. Energy 208 (2020) 430–444, https://doi.org/10.1016/j.solener.2020.08.015.
[35] D. Zhao, A. Aili, X. Yin, G. Tan, R. Yang, Roof-integrated radiative air-cooling system to achieve cooler attic for building energy saving, Energy Build. 203 (2019), 109453, https://doi.org/10.1016/j.enbuild.2019.109453.
[36] L. Carlosena, Á. Andueza, L. Torres, O. Irulegi, R.J. Hernández-Minguillón, J. Sevilla, M. Santamouris, Experimental development and testing of low-cost scalable radiative cooling materials for building applications, Sol. Energy Mater. Sol. Cells 230 (2021), 111209, https://doi.org/10.1016/j.solmat.2021.111209.
[37] M. Mirsadeghi, D. Cóstola, B. Blocken, J.L.M. Hensen, Review of external convective heat transfer coefficient models in building energy simulation programs: implementation and uncertainty, Appl. Therm. Eng. 56 (2013) 134–151, https://doi.org/10.1016/j.applthermaleng.2013.03.003.
[38] F.P. Incropera, D.P. Dewitt, T.L. Bergman, A.S. Lavine, Fundamentals of Heat and Mass Transfer, sixth ed., John Wiley & Sons, 2007. https://search.ebscohost.com/login.aspx?direct=true&AuthType=sso&db=cat03043a&AN=bupn.00223002&lang=es&scope=site&custid=s8433765.
[39] T.R. Oke, City size and the urban heat island, Atmos. Environ. 7 (1973) 769–779.
[40] Center For International Earth Science Information Network-CIESIN-Columbia University, Global Urban Heat Island (UHI) Data Set 2013, 2016. https://doi.org/10.7927/H4H70CRF.
[41] M. Kottek, J. Grieser, C. Beck, B. Rudolf, F. Rubel, World Map of the Köppen-Geiger climate classification updated, Meteorol. Z. (2006) 259–263, https://doi.org/10.1127/0941-2948/2006/0130.
[42] Meteonorm 7 (2017). www.meteonorm.com.
[43] R. Perez, P. Ineichen, E.L. Maxwell, R.D. Seals, A. Zelenka, Dynamic global-to-direct irradiance conversion models, Build. Eng. 98 (1992) 354–369.
[44] J. Feng, K. Gao, M. Santamouris, K.W. Shah, G. Ranzi, Dynamic impact of climate on the performance of daytime radiative cooling materials, Sol. Energy Mater. Sol. Cells 208 (2020), 110426, https://doi.org/10.1016/j.solmat.2020.110426.